



Scientific-Research Article

Mixed Convection and Radiation Heat Transfer in an Enclosure Filled with Unevenly Heated Plates at Different Configurations

Armin Sheidani¹, Sahar Noori^{2*}, Djavad Kamari³

1- Department of Mechanical Engineering, University of Polytechnic of Milan

2-3 Department of Aerospace Engineering, Amirkabir University of Technology

ABSTRACT

Keywords:

In this study, the effect of different configurations of three plates in an air-filled container, including vertical, horizontal and tilted, on coupled radiation and natural convection heat transfer has been numerically investigated. The cavity's side walls were kept at a constant temperature, while the upper and lower walls were thermally insulated. In addition, non-uniform temperature distribution was applied to each of the plates. Moreover, this research studied the effect of coupled heat transfer on flow separation and local Nusselt number. The flow separation on the heated plates due to the thermal gradients was captured, and the subsequent effects were discussed. Also, the results reveal two main flow patterns: separation of the convective flow and stretching of the clockwise vortex, which is created by combined heat transfer. It was also demonstrated that these flow patterns are the main ones responsible for variations in heat transfer. Also, it was demonstrated that the plate configuration plays a vital role in combined heat transfer as a horizontal placement of the plates may increase the Nusselt number variation along the plate up to 60 times compared to the vertical counterpart.

Nomenclature

Nu	Nusselt Number
CW	Clockwise
CCW	Counter Clockwise
DO	discrete ordinate method
Ra	Rayleigh Number
Re	Reynolds Number
Pr	Prandtl number
U,V	X- and Y-direction velocity components

Introduction

Cooling using air natural convection in a cavity has been of great interest due to its wide availability. In previous years, the air natural convection in cavities where a barrier creates more complicated flow patterns and radiation heat transfer affects the flow characteristics has won attention. This area of study has many industrial applications, such as solar panels, electronic devices, skyscrapers, HVAC systems, and power

1 Msc.

2 Associate Professor (Corresponding Author) **Email:** s_noori@aut.ac.ir

3 Research Assistant

DOI: [10.22034/jast.2023.357234.1127](https://doi.org/10.22034/jast.2023.357234.1127)

Submit: 23.08.2022 / Accepted: 05.03.2023

Print ISSN:1735-2134 Online ISSN: 2345-3648

plant flares, to name a few. In addition, the real-life applications associated with this configuration of plates which represents the interactive heating of electronic boards, is yet another reason for the conduction of this investigation. To illustrate, the configuration of the electronic boards embedded in the moving components of a device, especially those exposed to intense temperature gradients such as the fault detection robots used mainly in furnaces or deep underground sites, are prone to high thermal stresses, which may finally lead to their failure. Having said so, therefore, this study is aimed at shedding light on the effect of different configurations on the temperature distribution to provide the engineer with insight into the design of such components.

Saravanan and Sivaraj [1] investigated the effect of the presence of a hot plate in a cavity on simultaneous natural convection and radiation heat transfer. In this study, a plate was placed at vertical and horizontal positions, and the effect of the hot plate directly on the thermal field was studied. Various non-dimensional numbers govern the flow field subjected to combined radiation and natural convection. In this regard, Parkash and Singh [2] investigated the effect of such numbers on the combined heat transfer in a cavity. It was demonstrated that the Re number plays the most important role compared to the other non-dimensional numbers. In a similar study, Pordanjani et al. [3] showed that the Nu number and entropy production increase with the Rayleigh number. Owing to the importance of this matter, this has been investigated recently in many other studies [4]–[9]. Han and Baek [10] investigated the effect of the number of plates on the flow field in a cavity. In order to achieve this goal, two plates were placed at a particular distance from each other in the center of the cavity. It was reported that the amount of radiation in the place was significantly higher compared to that of the working gas. Yucel and Acarya [11], in a similar study, investigated the effect of the presence of two plates in a cavity on the flow pattern created by simultaneous natural convection and radiation heat transfer. It should be noted that such studies are conducted to simulate the cooling process of electronic devices.

Moutaouakil et al. [12] studied the combined heat transfer in a cavity filled with a wavy surface. It was shown that the radius of the wave is more effective than the number of waves to increase the

heat transfer. H. Bouali et al. [13] studied the effect of the angle of a cavity in which a cube had been placed symmetrically. The angles in this study were 60, -60 and 0 degrees concerning the gravity vector. The results suggest that when the effect of radiation is disregarded and for an inclination angle of 60 degrees the main mechanism of heat transfer was conduction both in vacant and occupied cavities. More interestingly, at an inclination angle of 0, the isotherms are horizontal, indicating the heat transfer mechanism is conduction, while when the cavity is filled with the rectangular object, the isotherms are inclined and convection plays a more decisive role. In the case of an inclination angle equal to -60, an opposite phenomenon was observed meaning that when the cavity is empty, the isotherms are distorted and when it is partitioned, the isotherms tend to be perpendicular to the gravity vector. Also, it was reported that when the inclination angle is reduced, the main heat transfer mechanism transmutes from conduction to single-cell convection which is mostly present at 0. Further, if the inclination angle is reduced even more to -60 the Benard convection will be the main responsible for heat transfer. It was also reported that the Nu number increases with the increase in the inclination angle. Furthermore, it was found that an increase in the temperature difference between the inner body and the walls leads to an increment in the average Nu number along the walls. Another finding of this study which is worthy of mention is that the ratio between the conductivity of the inner body and the working fluid can strongly affect the heat transfer mechanism. It was concluded that the increment of this ratio causes the natural convection to be weaker as the main portion of the heat transfer tends to occur by heat conduction through the inner body. Vivek et al. [14] conducted a study on coupled radiation and convection heat transfer in a tilted cavity. The tilt angle lied in a range varying from -90 to 90 degrees. It was found that in positively tilted cavities, the presence of radiation heat transfer does not affect the final velocity contours and only the temperature field undergoes some slight changes, however, in the case of a positive angle of tilting the radiation results in profound alterations in both temperature and velocity fields. It was concluded that the presence of radiation leads to higher flow circulation. In addition, the cold wall causes the moving fluid to lose heat, while the hot wall diffuses thermal energy to the convective flow. These two

phenomena are known as pre-cooling and pre-heating, respectively. It was also reported that in the case of positive tilt angles the main mechanism of heat transfer is pre-heating/cooling. However, when the tilt angle is reduced, or in other words, at negative tilt angles, the mechanism tends to come into existence through convective circulation. Moreover, it was illustrated that the interaction between radiative and convective heat transfer exists in the aspect ratio.

Shu et al. [15] investigated the thermal interaction between a cylinder and a cavity surrounding it, employing the DQ method. It was demonstrated that this numerical method is efficient enough to capture the weak flow structure in the domain. Jami et al. [16] made a numerical investigation to study combined heat transfer in a cavity whose central part had been filled with a cylinder. The fluid flow was simulated using the Lattice-Boltzmann method and the finite difference method to calculate the temperature field. It was reported that the average Nu number on the cold wall rises linearly as the temperature difference ratio increases, whereas an opposite trend was observed for the hot wall. Also, for temperature difference ratios greater than 40, the convective flow was mainly caused by the heat generated by the inner body. Lee et al. [16] studied the effect of the position of a cylinder in a cavity. In addition, immersed boundary method (IBM) was employed to calculate the flow characteristics. It was proven that the local Nu number along the cylinder surface and the cavity walls exist in the gap between them. It was reported that at low Ra numbers, the main mechanism by which heat transfer exists is conduction; the finest isotherms form near the narrower region between the cavity and the cylinder. Nevertheless, when the Ra number was increased by one order of magnitude, a phenomenon called a thermal plume formed on the top of the cylinder. This was attributed to the effects of buoyancy and natural convection, which are typical characteristics of higher Ra numbers. It was also found that when the cylinder traverses diagonally towards one corner of the cavity a vortex is separated, and two new vertices are formed in the narrower part of the cavity. Garoosi et al. [17] simulated the combined heat transfer in a Nano-fluid heat exchanger by a cavity filled with an array of cylinders. It was illustrated that by changing the geometry of the cavity from a rectangle to a triangle, the amount of heat transfer

per unit of time experiences a downward trend. Moreover, an optimum amount of Ra number was calculated at which the heat transfer rate hits its maximum amount. Yoon et al. [18] studied convection heat transfer at $Ra=10^7$ in a cavity with a cylinder whose location would be altered vertically. It was shown that depending on the position of the cylinder the heat transfer mode changes from a steady state condition to a transient one. They also specified an area in which the object's displacement did not result in the unsteadiness of the convective flow. It was demonstrated that when the cylinder is placed at a distance near the boundaries of the enclosure the narrow space leads to the unsteadiness of the fluid flow, and therefore pure Benard convection heat transfer comes into existence. Another important finding of this study was that when the distance between the cylinder and the cavity boundary is rather high, the natural convection is characterized by only one single frequency. However, when the distance increases, multiple frequencies appear. Zeitoun and Ali [19] investigated natural convection at different Ra numbers in an enclosure with sundry cross sections of geometries, which were rectangular and circular. It should be noted that the computations were performed by means of the finite element method (FEM). It was concluded that flow separation occurs at the top of the cavity when the aspect ratio increases. Also, it was reported that when the Ra number was increased, the thermal boundary layer thickness decreased at the side and lower walls of the enclosure. Nonetheless, at the upper surface of the cavity where the thermal plume is ascending, the increment of the Ra number has insignificant effects on the thermal boundary condition thickness.

Sieres et al. [20] numerically studied heat transfer in a triangle in the form of a right triangle. The main objective of this study was to study the effect of the tip angle alteration, and also, the presence or absence of radiation was investigated. It was shown that there is a direct relation between the average convective Nu number along the hot wall and the Ryleigh number. However, an opposite trend was reported for the relation between the average convective Nu number and the tip angle variation.

Additionally, it was found that the presence of radiation leads to higher convection velocity and as a result, higher value of the average Nu number.

Moreover, the effect of radiation was reported to be more significant at higher Ra numbers. Sheikholeslami et al. [21] investigated the combined heat transfer of a “Ferrofluid” in a ring-shaped cavity in the presence of a magnetic source. In order to perform the calculations, control volume-based FEM was employed. The results revealed that the Nu number rises with the increase in the Ra number. However, it was reported that there was an inversed relation between the Nu and Hartmann number. Bahlaoui et al. [22] studied the combined heat transfer in a cavity where an object was placed on the heated wall. The effect of several parameters, such as emissivity, the Re number and the object's location was investigated. The parameters were found to be effective in terms of increasing the heat transfer rate. It was also demonstrated that the presence of radiation leads to a more uniform temperature distribution. Moreover, it was reported that the radiation presence leads to a less convective Nu number.

Basak et al. [23] studied the effect of the thermal boundary condition of enclosure walls on natural convective flow by means of penalty FEM. They conclude that the non-uniform temperature distribution on the lower wall of the cavity leads to a higher heat transfer rate at the lower wall's central part than that of the uniformly heated wall. Also, the range of Ra numbers below which heat conduction was the main heat transfer mechanism was achieved. Corcione [24] studied the effect of thermal boundary conduction at the side walls of an enclosure on natural convection heat transfer. Aspect ratio and Ra numbers were other parameters whose effects were taken into consideration. It was also reported that the role of the unevenly heated lower wall rises into importance when the adiabatic side walls are replaced with temperature-constant ones.

Furthermore, it was found that over a particular amount of Ra number, the heat transfer from the side walls was independent of their boundary condition. Cianfrini et al. [25] conducted a study on natural convection in a tilted cavity. The effects of tilting angle Ra number were investigated in this study. It was concluded that for the sufficiently high value of the tilting angle, the heat transfer rate would be higher than that of the horizontal case. It should be noted that the range of tilting angle at which the heat transfer rate exceeds that of the horizontal one is highly dependent on the Ra number. Ayachi et al. [26] investigated combined

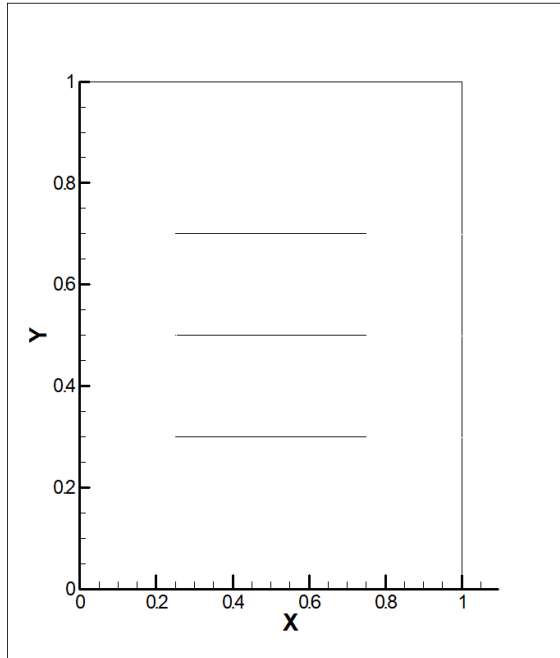
natural convection and radiation heat transfer in a cavity whose left wall experienced sinusoidal temperature variation throughout history. The effects of the constructing parameters of the sinusoidal temperature variation along with emissivity, Ra and Pr number were investigated. The results suggested that heat transfer increases considerably compared to the case in which the constant temperature distribution had been applied to the left wall. It was also reported that the phenomenon was observed in the case of radiation presence of resonance. Ridouane et al. [27] undertook an investigation on mixed heat transfer in the cavity with the lower heated lower wall. The results revealed that the emissivity decreases the range of the Ra number in which the problem can be considered steady. Kim et al. [28] studied natural convection in a cavity filled with a cylinder. The influence of the temperature distribution of the lower wall of the cavity on the thermal and flow field was investigated at different Ra numbers. It was found that there was a direct relation between the Ra number and non-uniformity of the isotherms and streamlines. In other words, more convection cells were observed in the cavity when the Ra number was increased.

Having considered the previous studies, one can come to the conclusion that the simultaneous interaction of different plates and the tilting angle has remained intact. In fact, the presence of other plates in a cavity affects the combined heat transfer. To illustrate, the restricted area between the plates leads to a change in Re number and inevitably in convective heat transfer rate. On the other hand, the amount of radiation heat transfer is unquestionably affected by the other radiative heat sources. In addition, in industrial applications of this phenomenon i.e. combined convective and radiation heat transfer in a cavity, more than one plate exists, and their direction with respect to the cavity walls is not always horizontal or vertical. As a result, in this study, the effect of the presence of a higher number of plates and their inclination will be investigated to simulate this phenomenon more precisely.

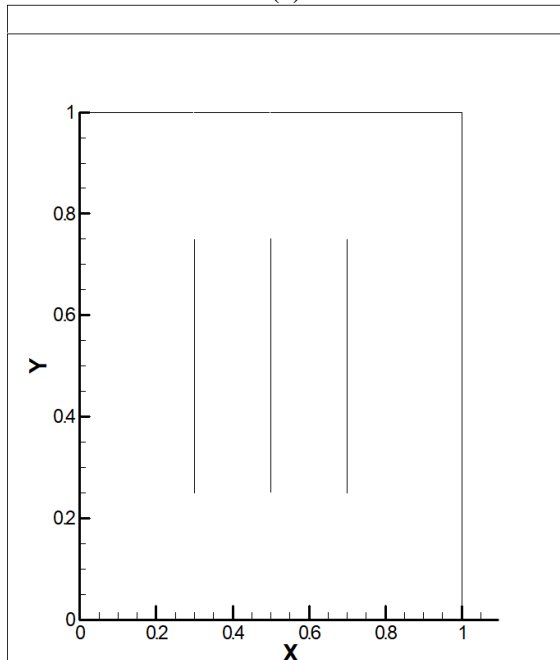
Problem description

The schematic figure of the geometry for different cases has been presented in Fig.1. As illustrated, three cases will be studied. In the first case, the plates are placed in a horizontal configuration. In the second case, the plates are vertical, and in the

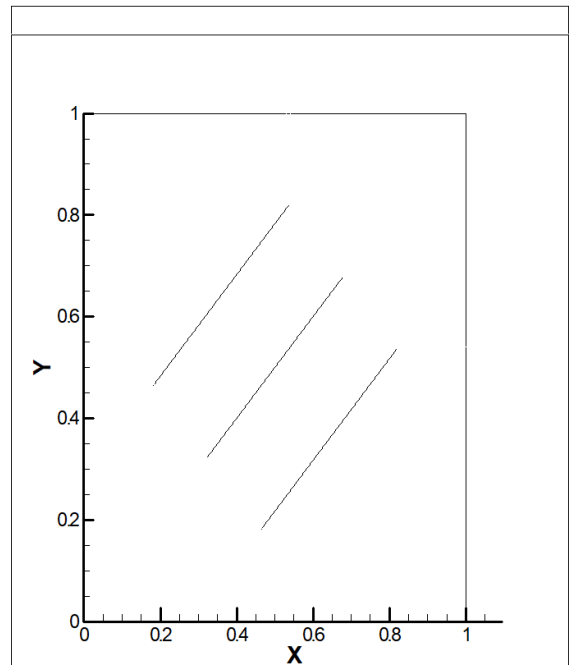
third one, they have been tilted around their center of gravity. Furthermore, as demonstrated in Fig.1, the side walls were kept at a constant temperature equal to 293.15K and the upper and the lower walls were assumed to be adiabatic.



(a)



(b)



(c)

Fig.1- Three Plates configurations (a) horizontal case (b) vertical case (c) tilted case.

The non-uniform temperature distribution was assumed to be a linear function of the position along the plate. The temperature distribution is calculated according to the following equation.

$$T(s) = \left(\frac{T_{hot1} + T_{hot2}}{2} + \left(\frac{Length}{h_{plate}} \right) \left(\left(\frac{T_{hot1} - T_{hot2}}{2} \right) \left(1 - \frac{2s}{Length} \right) \right) \right) \quad (1)$$

Where s is the location of the point at which the non-uniform temperature is calculated. It is worthy of mention that in some cases, the slope of linear temperature distribution in Eq.1 was set to be zero. As a result, the plate temperature was uniform and equal to 308.15k.

In order to study the effect of the non-uniform temperature distribution on the plates, four cases were studied for each plate configuration. At first, no temperature distribution was applied to the plates to investigate no-temperature gradient effects. Following this, a temperature gradient was applied to each plate. In order to be able to recall the cases easier, in Table.1 a name has been attributed to each one.

Table1- case names

Configuration	Plate with unevenly temperature distribution	Name
Horizontal	None	H-1
	Lower	H-2
	Middle	H-3
	Upper	H-4
Vertical	none	V-1
	middle	V-2
	side wall	V-3
Tilted	None	T-1
	Lower	T-2
	Middle	T-3
	Upper	T-4

Numerical approach

As mentioned before, the air was regarded as a working fluid whose properties were assumed to be constant except for density and viscosity due to the buoyancy effect. Also, the opaque grey boundary condition was applied to the walls and the plates. Furthermore, it was assumed that the flow is laminar and therefore the governing equations i.e. momentum and energy equations, will be as follows:

$$\frac{\partial u}{\partial x} + \frac{\partial v}{\partial y} = 0 \quad (2)$$

$$\begin{aligned} \frac{\partial u}{\partial t} + u \frac{\partial u}{\partial x} + v \frac{\partial u}{\partial y} \\ = -\frac{1}{\rho} \frac{\partial P}{\partial x} \\ + \nu \nabla^2 u \end{aligned} \quad (3a)$$

$$\begin{aligned} \frac{\partial v}{\partial t} + v \frac{\partial u}{\partial x} + v \frac{\partial v}{\partial y} \\ = -\frac{1}{\rho} \frac{\partial P}{\partial y} \\ + \nu \nabla^2 v + g\beta(T - T_0) \end{aligned} \quad (3b)$$

$$\begin{aligned} \frac{\partial T}{\partial t} + u \frac{\partial T}{\partial x} + v \frac{\partial T}{\partial y} \\ = \alpha \left(\frac{\partial^2 T}{\partial x^2} + \frac{\partial^2 T}{\partial y^2} \right) \end{aligned} \quad (4)$$

In order to include the effect of radiation, Eq.5 which represents the radiative transfer equation must be taken into account. In order to solve Eq.5, the DO method was employed.

$$\begin{aligned} \nabla \cdot (I(r, s)s) + (a + \sigma_s)I(r, s) = an^2 \frac{\sigma T^4}{\pi} - \beta I(r, s) + \frac{\sigma_s}{4\pi} \int_0^{4\pi} I(r, s)\Phi(s, s')d\Omega' \end{aligned} \quad (5)$$

Where a, σ , r and s are the absorption coefficient, Stefan-Boltzmann constant, distance from the radiative heat source and the direction of the radiation propagation. As a matter of fact, the main difficulty regarding the resolution of the radiative transfer equation is the third term on the RHS including an angular integral. In order for this term to be discretized, the discrete ordinate (DO) method was employed. In this method, the solid angle is divided into some discrete angles. As a result, the integral part can be discretized over the spatial angle and the governing equation changes as follows:

$$\begin{aligned} \int_0^{4\pi} I(r, s)\Phi(s, s')d\Omega' \\ = \sum_{j=1}^n \omega_j I(r, s_j)\Phi(s_j, s_i) \end{aligned} \quad (6)$$

Where ω_j is the weighting coefficient, generally, non-grey DO model calculates the RTE for different radiation spectra. However, as the radiative transfer equation is solved only for black body emission, the number of bands was set to zero.

In order to assess the results a Nu number of the plates was calculated. It should be noted that in the grid independency study, the average Nu number was used. The local Nu number was calculated on each plate to better understand the combined heat transfer phenomenon on a plate. The equations by which local and average Nu number was calculated has been presented in the following respectively:

$$Nu_x = \frac{h_x x}{l} \quad (7)$$

$$Nu_{ave} = \frac{1}{l} \int_0^l Nu_x dx \quad (8)$$

In order to observe the flow pattern caused by combined heat transfer, stream function needs to be plotted. In fact, in the following sections dimensionless stream function has been plotted according to the equation presented below.

$$U = \frac{\partial \Psi}{\partial Y} \quad (9a)$$

$$V = -\frac{\partial \Psi}{\partial X} \quad (9b)$$

In the following, to perform a grid independency study, three different meshes containing 120000, 240000, and 435000 cells were generated and the Nu number of each mesh was plotted in Fig.2. It should be noted that the simulations were performed in Ansys Student Fluent v.19. In this regard, a two-dimensional laminar solver was opted due to the low Re number associated with the natural convection in this study. In addition, a semi-implicit method for pressure-linked equations (SIMPLE) and a second-order discretization scheme for the convection term was employed. Moreover, the density of the gas was calculated according to ideal gas relations to account for the compressibility of the convective flow. As it is evident in Fig.2 the Nu number of all of the three meshes yield almost the same results.

Plate	120000	240000	435000
Lower	25.40675	25.433798	25.44160
Middle	20.17412	20.194474	20.20347
Upper	31.05761	31.305669	31.31726

Fig.2- Grid independency study.

In addition to the grid independence study, an angular division independence investigation needs to be carried out due to the employment of the DO method. As seen in Fig.3, the DO technic was implemented based on 2,3,4,6 and 8 divisions both in θ and ϕ direction. The result reveals that the average Nu number for all of the cases is almost equal. As shown in Fig.3 when the spatial angle division number exceeds six, the maximum

amount of average Nu number will be less than 7 percent. As a result, ϕ division was set to be 6.

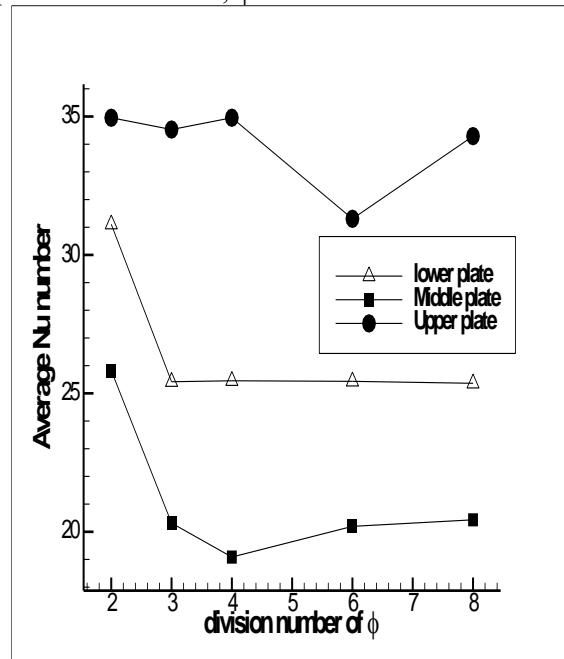


Fig.3- Spatial angle independency study

Results and discussion

The computations regarding fluid flow and heat transfer equations were performed for a Ra number equal to 10^7 . The temperature contour created by pure natural convection around a single plate has been presented in Fig.4. It is evident the results show good agreement with that of [1]. In addition, in Table 2 the Nu number on the cavity wall has been reported. As seen in table 2 a very good agreement between the results can be observed.

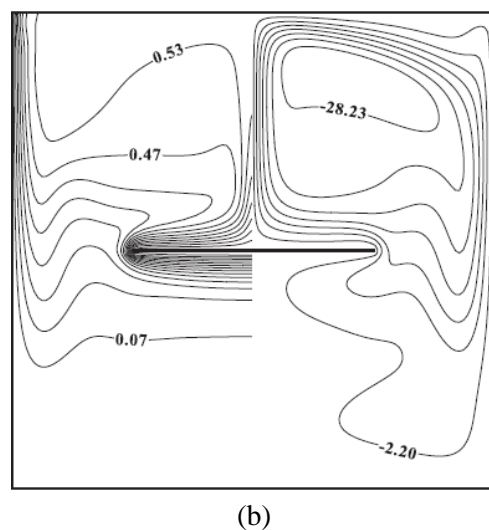
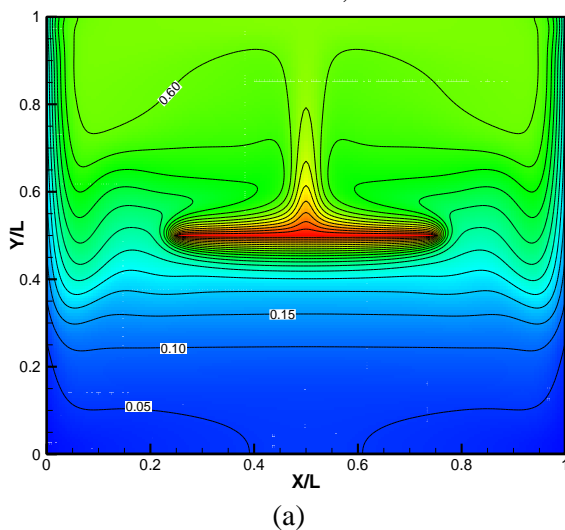


Fig.4- Temperature Contour in the Cavity under the influence of pure convection (a) Current Simulation (b) Sarvanan and Sivaraj [1].

Table 2- Verification of the numerical approach by comparing of Average Nu number on the left wall.

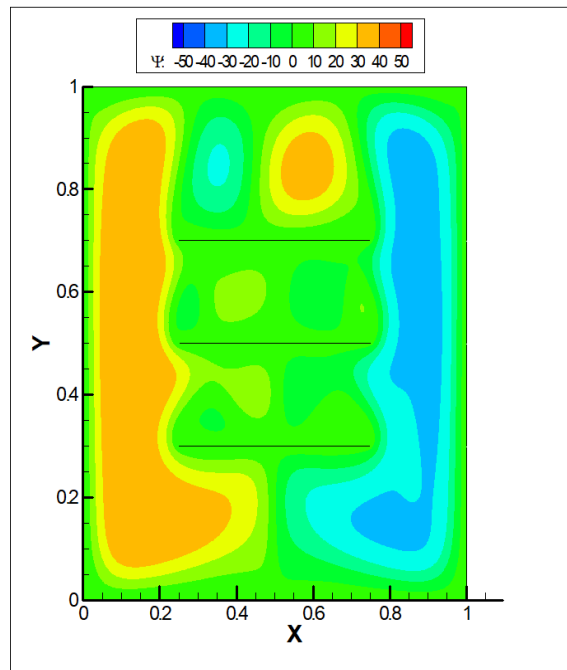
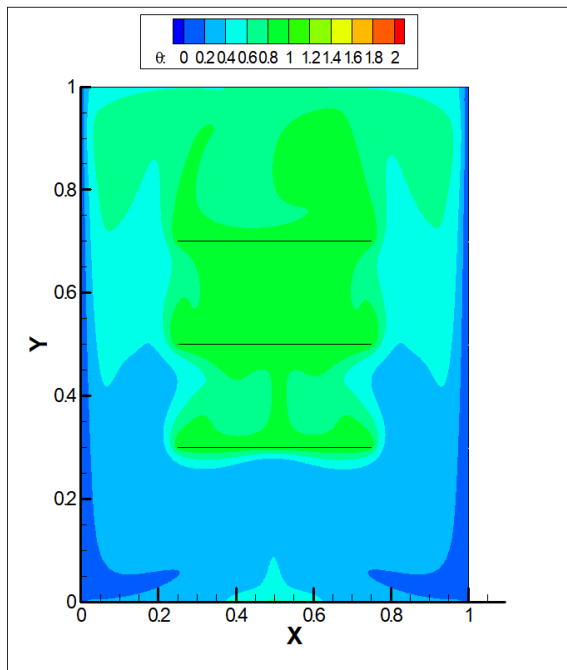
Present study	Results of Ref.[1]
9.65	8.76

Horizontal plates

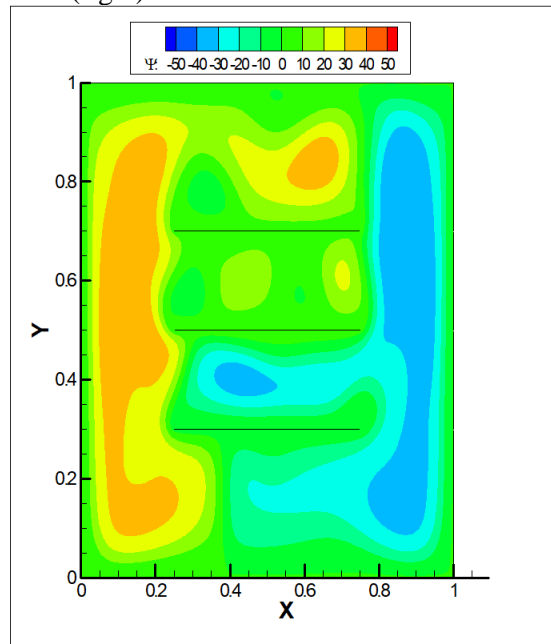
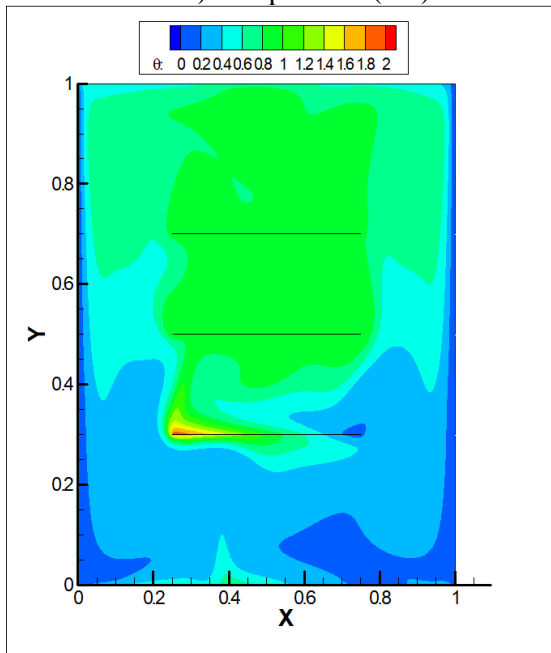
Following this, the effect of the presence of three plates in the horizontal configuration in the cavity will be investigated. The stream function and temperature distribution contours of different cases have been presented in Fig.5. As shown in Fig.5a, when all of the plates possess uniform temperature distribution along their length, the stream function and temperature distribution contour is also uniform. Additionally, a CW massive vortex is seen on the right-hand side of the cavity while another CCW one with the same size and magnitude is rotating on the left part of the domain indicating that unlike the case with only one plate in which natural convection occurred only on the top of the plate, the natural convection is in progress in the whole domain but separately on the sides of the cavity and somehow between the plates. The pair of side vertices also indicates that the plate's edges and the radiation emitting from spaces between them act like a hot wall bringing about natural convection. This observation is also attributed to the fact that the mechanical resistance of the plates prevents the formation of a vortex covering the whole cavity. Nevertheless, as it is discernable in Fig.5b when a non-uniform thermal boundary condition is applied to the lowest plate the uniformity of the contours undergoes disruption in the vicinity of the lowest and highest plates. However, the total trend of stream function distribution in areas far from the plate with linear temperature distribution remains approximately symmetrical.

Another point which is worthy of mention is that when a non-uniform boundary condition is applied to one of the plates the CW vortex is stretched towards the plate with non-uniform, while the CCW vortex extends its domain to the furthest plate. This is due to the fact that as the left side of the plate possesses the highest temperature in the cavity, the natural convection between the plates begins at this point. On the other hand, the temperature of the plate decreases along the positive direction of the horizontal abscissa. As a result, the vortex formed by natural convection tends to move from the left to the right side of the

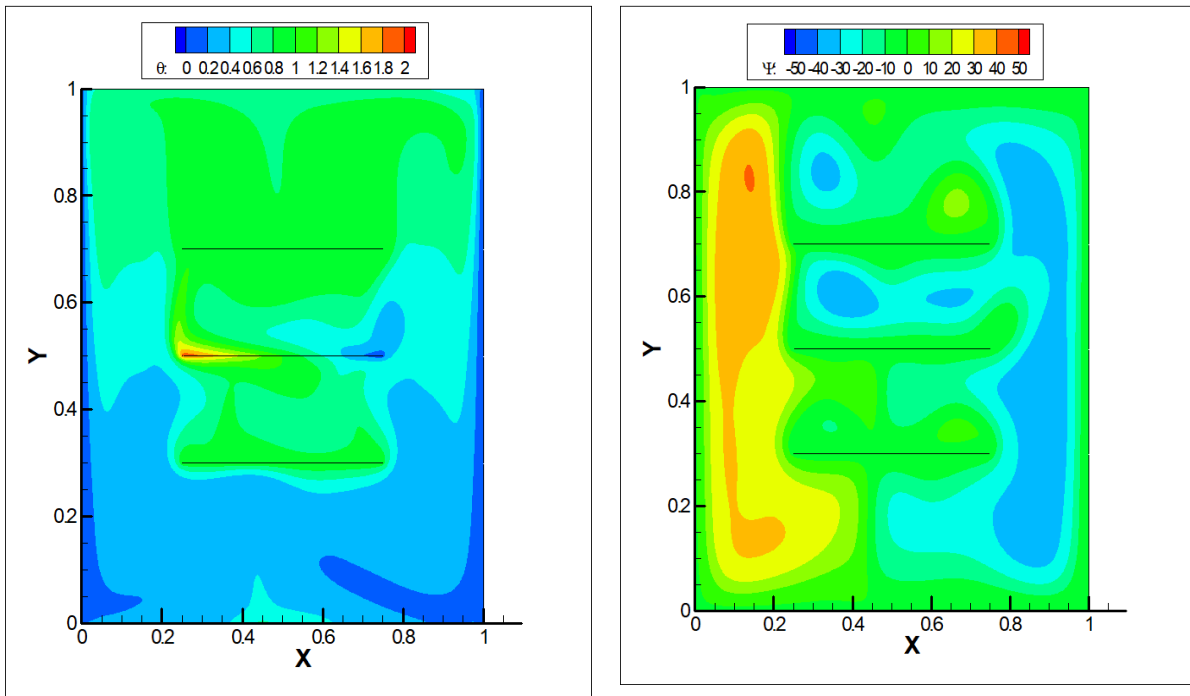
cavity. More importantly, as the vortex moves from left to right it experiences a temperature drop. Therefore, the vortex tends to be detached from the plate surface and reaches an area with higher temperature which, according to the temperature contour in Fig.4b, has been located on the left and upper part of the plate. Consequently, the CW vortex is stretched into the space between the plate with non-uniform temperature distribution and the plate above. Moreover, in Fig.5b a stretched vortex is observed on the top of the upper plate. This is attributable to the position of CW and CCW vertices intersection at the bottom of the lowest plate. Because in the case of non-uniform temperature distribution on the lowest plate, the amount of maximum temperature shifts towards the end of the plate with the highest amount of temperature. This peak of temperature on the lowest wall of the cavity is responsible for the natural convection and therefore vortex generation. Moreover, the vortex generated on each side of the cavity is able to cover a particular distance more or less equal to the case in which uniform temperature distribution had been applied to the plates. As a result, the CCW vortex can cover the whole area above the upper plate as it has been formed near the left side of the cavity. It is quite evident that when the temperature is non-uniformly distributed on the lowest plate the temperature peak on the lowest wall of the cavity is inclined towards the maximum temperature of the lowest plate. One may put down this observation to the fact that in case of the uniform temperature distribution the middle part of the lowest cavity wall receives the most amount of irradiance, while when the temperature distribution is not uniform the area near the hottest part of the plate receives more energy compared to other parts of the plate. Thus, at this point, the natural convection vertices begin to grow. As seen in Fig.5b to 5c the uniformity of the stream function distribution is completely lost when all of the plates experience non-uniform temperature distribution. Another point which is worth mentioning is that natural convection is mostly present on the upper plate as this mechanism occurs due to the difference in the density.



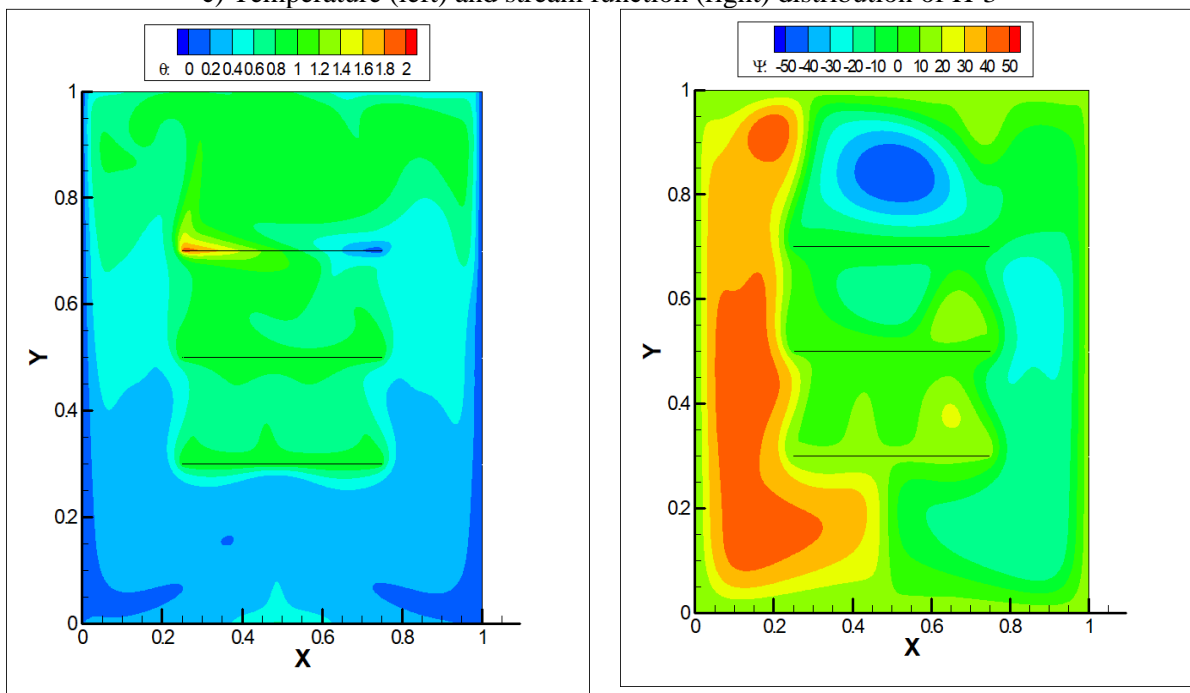
a) Temperature (left) and stream function (right) distribution of H-1



b) Temperature (left) and stream function (right) distribution of H-2



c) Temperature (left) and stream function (right) distribution of H-3



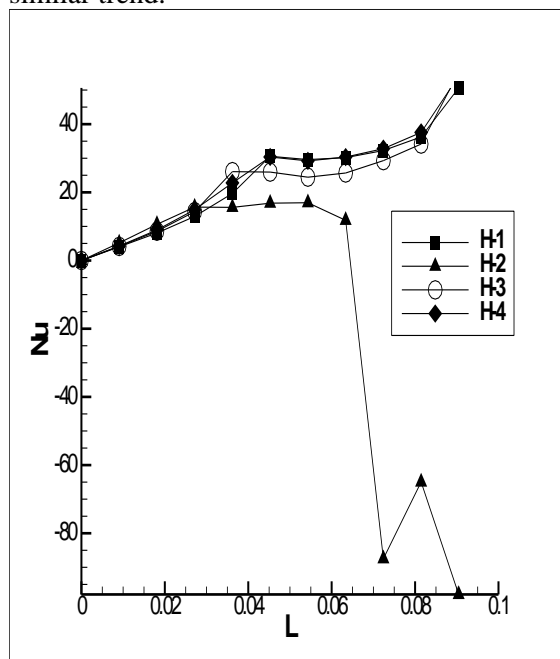
d) Temperature (left) and stream function (right) distribution of H-4

Fig.5- Temperature and stream function contour of the horizontal plates.

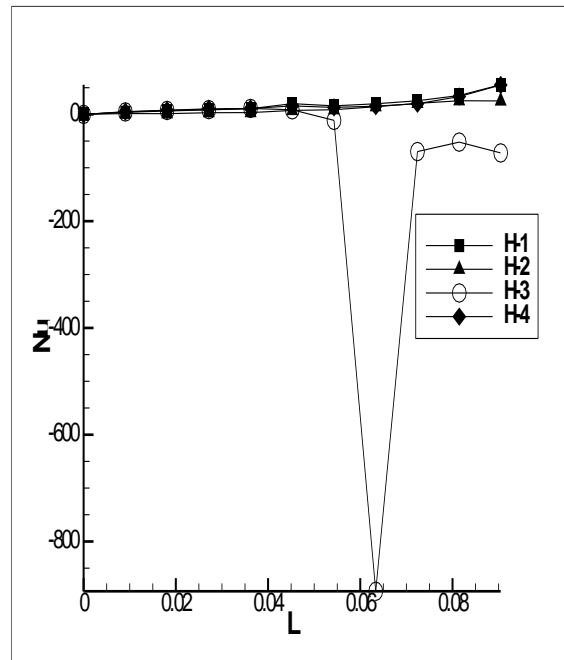
The local Nu number of the plates has been presented in Fig.6. It is clear that when vortex stretching occurs the local Nu drops sharply. Moreover, in the cases in which non-uniform temperature distribution has been applied to, steeper curves can be observed. Furthermore, except for the plate with uneven temperature distribution, other plates demonstrate a similar

trend in terms of the local Nu number growth. It is observed that in all of the cases with non-uniform heated plates, the Nu number undergoes a change in heat transfer direction which is due to the separation. However, the sharpest drop in Nu number occurs in the H-3 case. The reason of this observation can be understood by considering the stream function contour of this case. As seen the

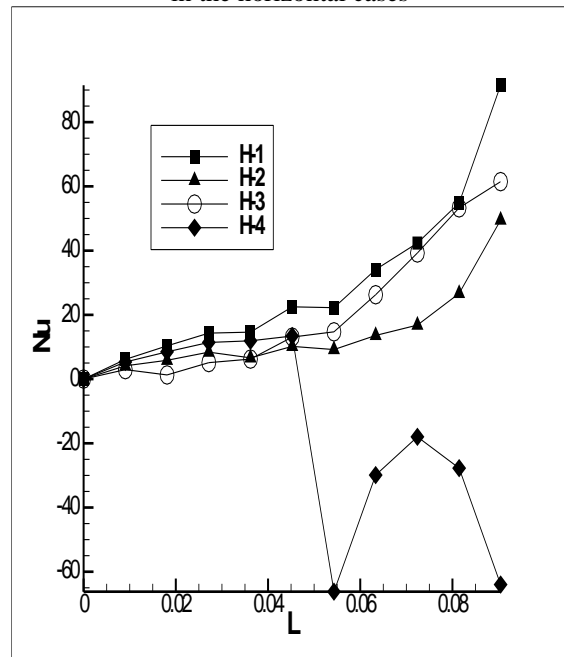
strongest separated vortex forms in the H-3 case. This is due to the fact that the separated convective flow reattaches to the massive convective vortex located at the two sides of the cavity leading to strengthening the separated vortex. In addition, on the lower side of the middle plate a vortex, which is stretched to almost halfway of the middle plate, is observed. The outcome of these two vortices will be a dramatic increase in the local Nu number. In the H-4 case, an isolated separated CW vortex can be observed on the top of the upper plate. As it can be witnessed, this vortex is disconnected from the side convective vortex. As a result, reinforcement of this vortex cannot come into existence due to being isolated. Therefore, the H-4 case experiences the lowest amount of Nu number compared to all other cases. H-2 case a very similar trend to that of the H-3 case can be observed. However, the Nu number of the H-3 case is far more than that of the H-2 case. This observation can be explained by regarding the fact that in the H-3 case, both the upper and the lower vertices are confined in an area whose cross-section is smaller than that of the H-2 case. Nevertheless, the affinity of all of the cases in horizontal configuration is that when a non-uniform temperature distribution boundary condition is applied to one of the plates the local Nu number undergoes a sharp drop, while other plates which are evenly heated follow a similar trend.



a) Local Nusselt number variation of the lower plate in the horizontal cases



b) Local Nusselt number variation of the middle plate in the horizontal cases



c) Local Nusselt number variation of the upper plate in the horizontal cases

Fig.6- Local Nu number of the horizontal case.

In order to have a broader view of the physics behind this phenomenon, the average Nu number of the plates in each case has been presented in Fig.8. It is evident in the figure below that in the case of evenly heated plates, the amount of average Nu numbers for all of the plates are of the same order lying in the vicinity of a Nu number equal to 20. Nevertheless, the average Nu number of the upper plate is slightly more than that of the others.

On the other hand, when a plate undergoes non-uniform temperature distribution, the average Nu number of that plate will exceed that of the other ones however staying in the same order as other plates except for the middle plate. As seen in Fig.8, when a non-uniform temperature boundary condition is applied to the middle plate, the average Nu number rises to a maximum amount which is 5 orders of magnitude more than that of the other plates. This observation implies that the vortex stretching as a result of thermal separation affects the middle plate more than other plates. This observation can be attributed to the fact in the case of horizontal configuration, the separated flow will be reattached to another vortex resulting in strengthening the vortex. As the separated vortex is bounded between the two upper and lower plates the velocity of the vortex increases and therefore the heat transfer rate increases significantly.

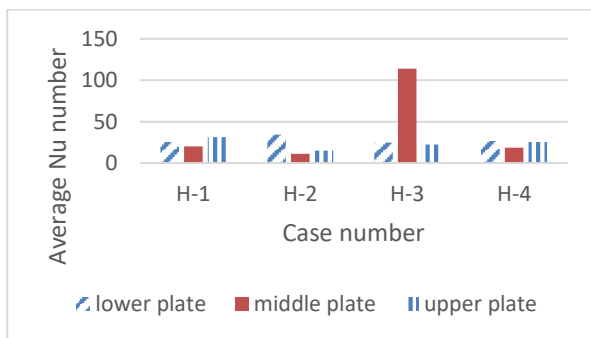
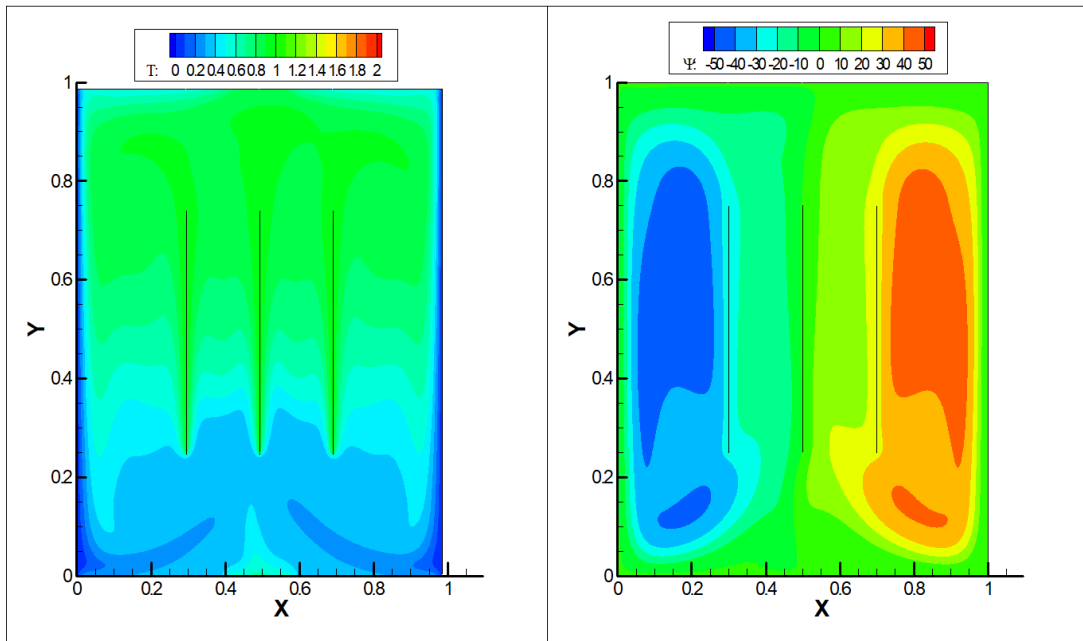


Fig.7- Average Nu number of the cases H1 to H-4.

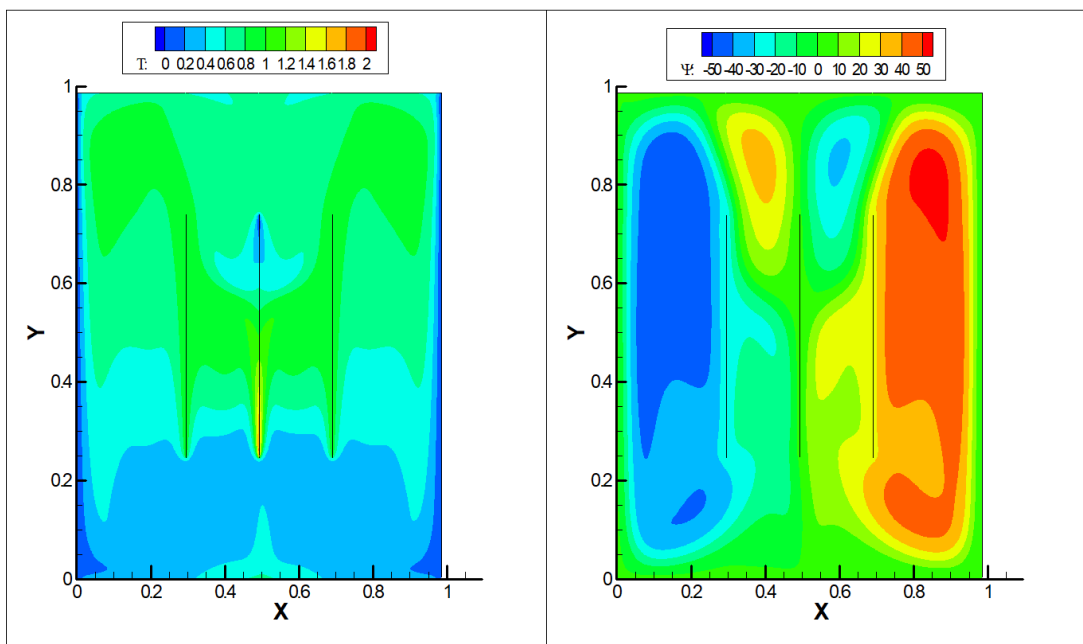
Vertical plates

In this case, phenomena which are similar to that of the previous case are observed. To illustrate, as seen in Fig.8a, when there is a uniform temperature distribution on all of the plates the flow stream distribution is also uniform in the whole domain. However, when a non-uniform thermal boundary condition is applied to the plates the symmetry of the temperature is destroyed. Furthermore, similar to the horizontal case a CW and a CCW vortex are present at the two sides of the cavity. These two vortices are the result of the hot plates at the sides of the domain creating vortices which are typical of convective flows. In

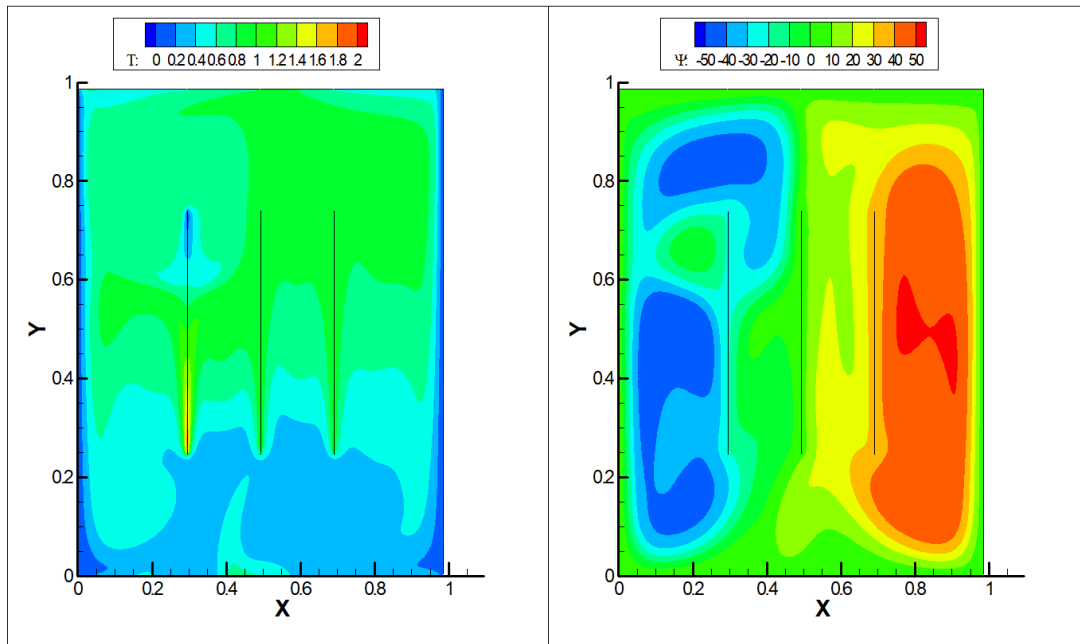
addition, between the plates still, some effects of natural convection are observed. However, unlike the horizontal case, the vertices at the sides of the cavity are not stretched to the bottom of the lower plate but the vortex generation where the temperature of the lower wall is maximum is observed. Nevertheless, when the non-uniform thermal boundary condition is applied to one of the side walls, as seen in Fig.8b, the boundary layer of the rising convective undergoes separation which is in total agreement with that of the [1]. This is attributed to the fact that as the convective flow rises, it undergoes a temperature drop. Therefore, the flow tends to detach and reattach where the temperature is higher. More importantly, as illustrated further, this phenomenon causes the Nu number to drop sharply at the point of separation. It should be noted that due to symmetry the result of the numerical simulation related to the left wall non-uniform temperature distribution has not been presented. It is also worthy of mention that the separated vortex is stretched towards the space between the right and the middle plate. This phenomenon occurs owing to the formation of the separated vortex and therefore reducing the area of the CW vortex propagation. The reduction in the cross-section area of the CW vortex movement leads to an increase in its momentum and as a result, the vortex covers a larger area. In Fig.8c, the temperature and stream function contours of the case in which the non-uniform thermal condition has been applied to the middle plate are presented. It is evident that the convective flow separation happens on both sides of the middle plate because of the reason mentioned earlier. However, as the separated vortex is large enough to block the whole area between the plates the vortex stretching phenomenon is not observed in this case. Since the separation happens at both sides of the middle plate, the Nu number, as shown further, will be the lowest compared to other cases.



a) Temperature (left) and stream function (right) distribution of V-1



b) Temperature (left) and stream function (right) distribution of V-2

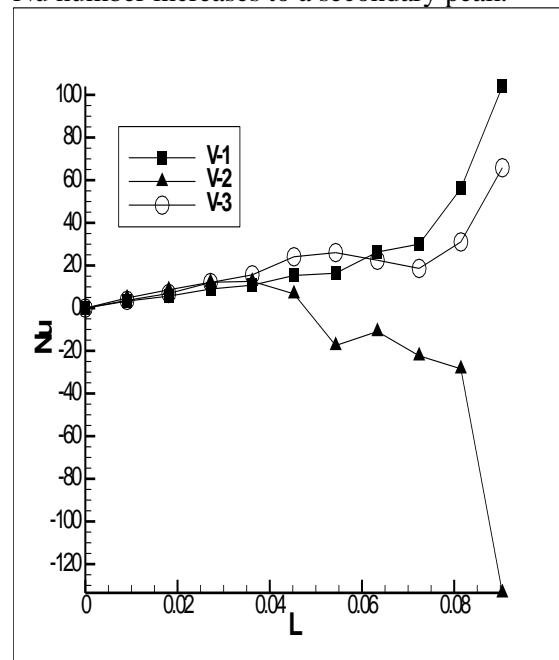


c) Temperature (left) and stream function (right) distribution of V-3

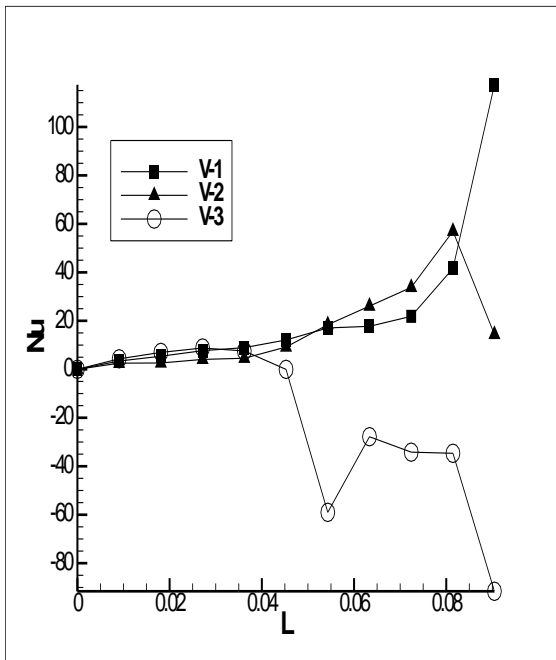
Fig.8- Temperature and stream function contour of the vertical plates.

The local Nu number of the plates and the walls have been presented in Fig.9. It is evident that at points where separation of the convective flow occurs the local Nu number drops sharply to a negative number. This is due to the fact that at this point, the heat transfer occurs in the area between the plates where separation does not exist or is less intense. As a result, the flow experiences a reverse heat transfer leading to a large negative amount of local Nu number. Similar to the horizontal configuration of the plates, the main convective vertices are located at the two sides of the cavity. On the other hand, because of the geometrical constraints of this case, reattachment of the separated vertices is not as feasible as it is in the vertical configuration case. Hence, the vortex strengthening is not as intense as it is in the horizontal configuration and the peak of the local Nu number curve is much lower compared to that of the horizontal case. Unlike the horizontal configuration case, when a non-uniform temperature distribution is applied to the middle plate, the side plate also sees a drop in the Nu number. This stems from the pair of separated vertices on the top of the middle plate. The vertices are large enough to block the major part of the convective flow and therefore, the heat transfer rate decreases. Another point which is worthy of mention is that in the V-3 case, a secondary peak can be observed after it plummets to its minimum amount. This is attributed to the vortex stretching

of the side convective towards the area confined by the middle and the side plate. As a result, the local Nu number increases to a secondary peak.



a) Local Nusselt number variation of the middle plate in the vertical cases



b) Local Nusselt number variation of the side plate in the vertical cases

Fig.9- Local Nu number of the vertical case.

In Fig.10 the average Nu number of the plates in vertical configuration has been presented. As illustrated, overall, the introduction of non-uniform temperature distribution to the plates does not cause the average Nu number to change significantly as what was observed in the horizontal configuration especially, for the middle in the H-3 case. As mentioned before this is due to the fact that in the horizontal case, the separated flow reaches a vortex front placed at one side of the plate leading to vortex strengthening and therefore higher heat transfer. Nonetheless, in the vertical case, the reattachment of the separated flow to the mainstream of the convective flow vertices is more difficult due to the geometrical constraints. On the other hand, the affinity between the vertical and the horizontal configuration is that when a non-uniform temperature distribution is applied to one of the plates, its average Nu number exceeds that of the other ones. As illustrated before, this is because of the separation associated with uneven temperature distribution.

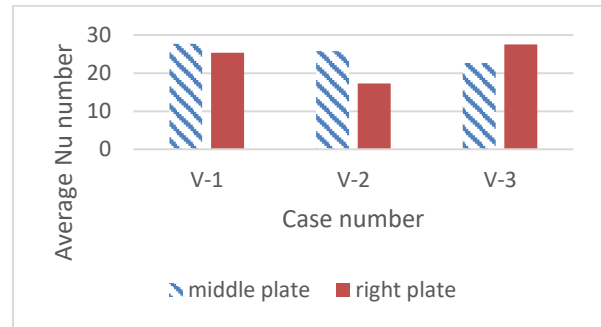


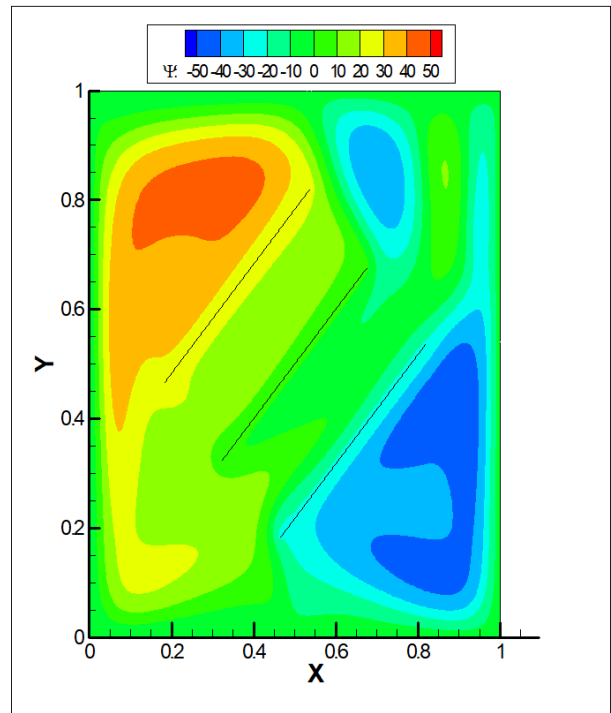
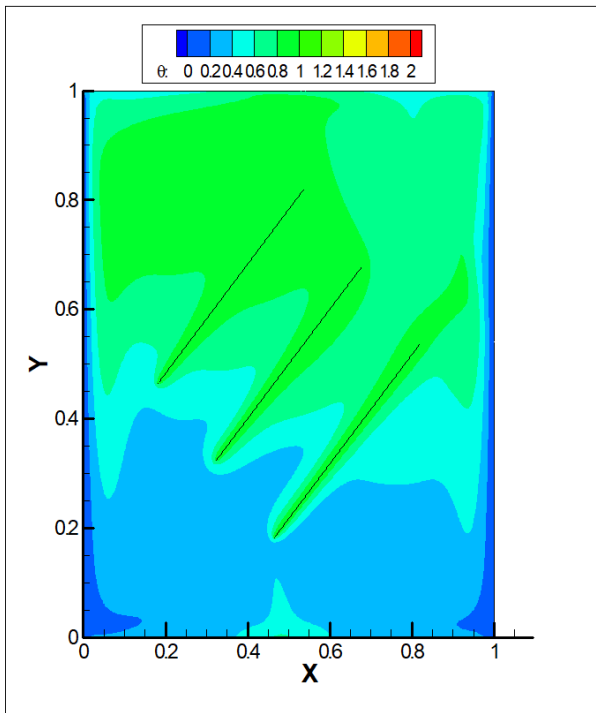
Fig.10- Average Nu Number of the cases V-1 to V-3.

Tilted plates

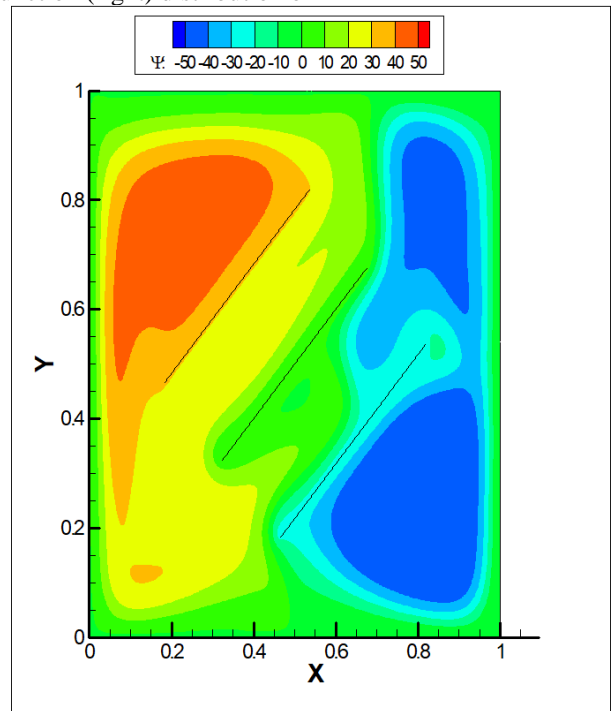
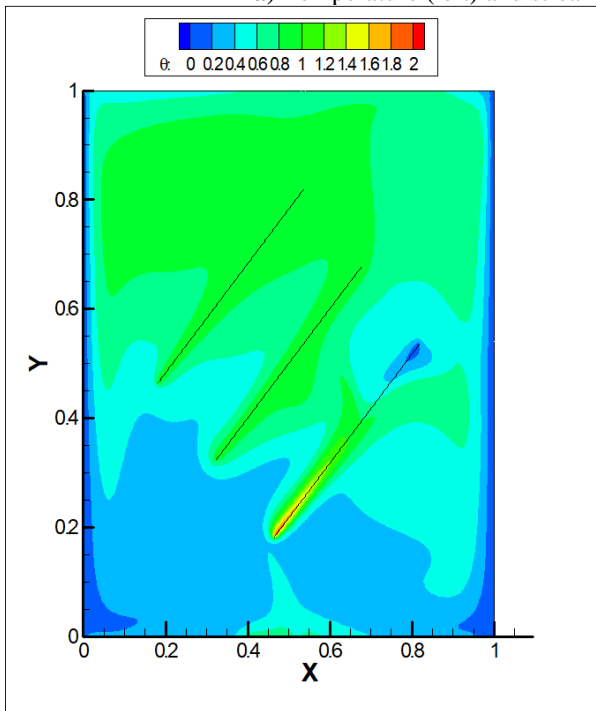
In Fig.11 the temperature and the stream function contours of the tilted plates have been presented. Similar to the previous cases, when a uniform temperature distribution exists on the plates the stream function contour seems to be symmetrical. In addition, in this case, there are two CCW and CW on the upper and the lower plates respectively, referring to the existence of the natural convection caused by the plates. In addition, the temperature contour of the uniform case, similar to the previous ones, is characterized by the increment of the temperature amount in the positive direction of the Y axis. This is due to the fact that in natural convection, the warmer front tends to be placed on the upper part of the colder part due to the dependency of density on temperature. In Fig.11b the contours of the case with a non-uniform temperature distribution on the lower plate have been presented. When an uneven temperature distribution is applied to the lower plate, an interstitial mode, which is a phenomenon between the vertical and the horizontal case, comes to existence. In other words, in this case, the two main observations of the previous cases i.e. vortex stretching towards the plate with non-uniform temperature distribution and separation of the convective flow typical of the horizontal and the vertical respectively case is observed. This is attributed to the fact that when the convective flow is propagating along the lower plate the presence of the temperature difference between the plate and the cavity walls is felt and as a result, the convective flow tends to be separated towards the wall with higher temperature. On the other hand,

due to the temperature difference between the plates the CCW vortex is separated and joins the warmer front. Detailed explanations of these phenomena have been presented in the previous cases. As a result of the interstitial mode of the convective flow, the flow characteristics will be in an intermediate amount between the vertical and the horizontal case. Hence, the separation is not that intense and the stretching phenomenon is not that extensive. This leads to a lower amount of the local Nu number drop as it is evident in Fig.11. In Fig.11c the contours of the case in which the uneven temperature distribution is applied to the middle plate have been presented. It is evident that there are two symmetrical vertices on the upper of the middle which is attributable to the fact that the convective flow between the middle and the other plates experiences a temperature drop and it tends to join the warmer front. However, the CCW vortex which has been located on the lower part of the middle plate is somehow stronger than the upper one. Moreover, the stretching of the upper CCW vortex in the domain between the middle and the lower plate is more intense compared to what happens between the upper and the middle plate. This is due to the fact that between the lower and the middle plate, the lower one is responsible for natural convection, while between the lower and the upper plate, natural convection is caused by the middle plate. Therefore, as seen in Fig.11c, the convective forms later in the space between the middle and the lower plate as the temperature at the left tip of the middle is higher than that of the lower one and obviously convective flow cannot be induced in the direction of the gravity vector. Thus, convective flow is generated where lower possesses a higher temperature which is further compared to that of the space between the middle

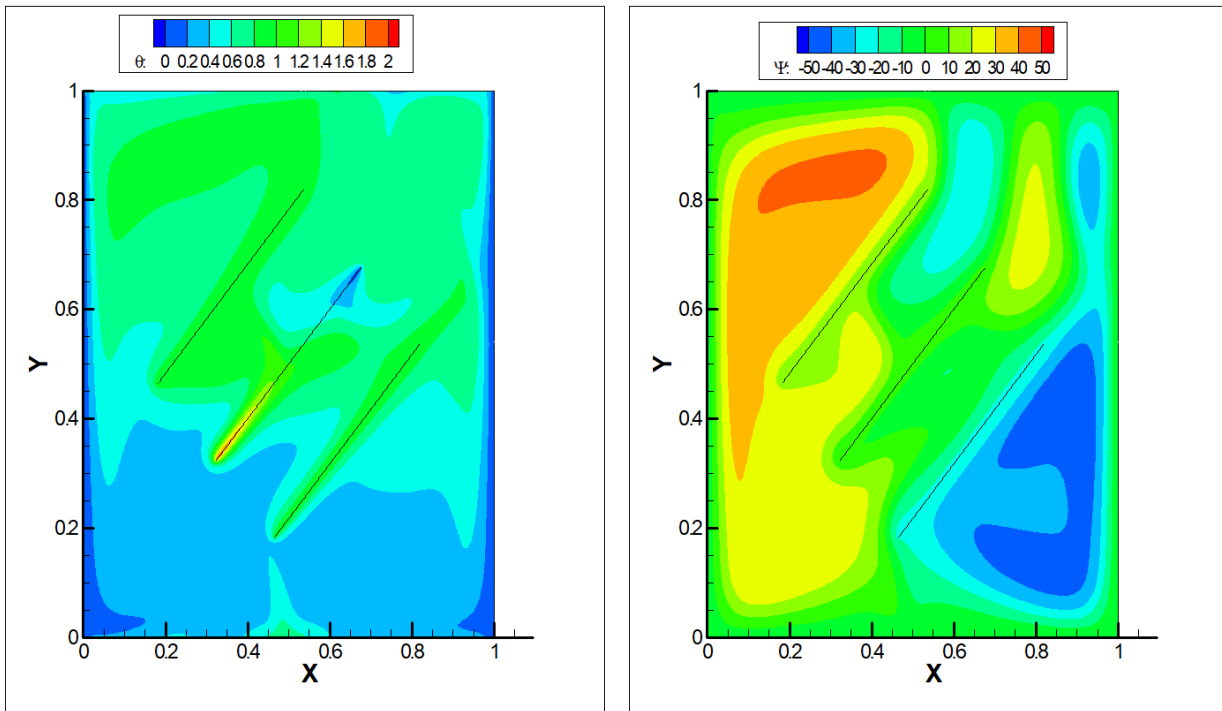
and the upper plate. This delay in the convective flow formation leads to more stretching of the upper vortex due to the lack of resisting vertices at that region. Also, the reason behind the stronger vertices between the middle and the lower plate is attributed to the fact that the separated flow in this region is confined between the separated convective flow in the area between the middle and the upper plate and also the lower CW vortex in the cavity. The confinement leads to a lower cross-section in which the lower separated convective can propagate and as a result, it leads to a higher velocity of this vortex. In Fig.11d the temperature and the stream function contour of the case in which the upper plate possesses non-uniform temperature distribution have been presented. It is observed vividly that the main part of the convection heat transfer happens in the area between the upper and the middle plates. As the temperature drops alongside the upper plate, the convection heat transfer occurs mainly by the middle plate. The separation of the convective flow between the plates is also discernable. In fact, one may expect to observe similar trends in both T-2 and T-4 cases due to the symmetry of the system. However, an opposite trend is seen. In the T-2 case, there is a rather small CW vortex below the lower plate while in T-4 no convective flow above the upper plate is observed. This is because the radiation heat transfer at the hotter tip of the plates leads to a temperature increment of the cavity walls near the hottest end of the plates. In both cases, this increment leads to hotter cavity walls. However, due to the fact that natural convection happens only to the opposite side of the gravity vector, convective flow is present only around the lower plate.



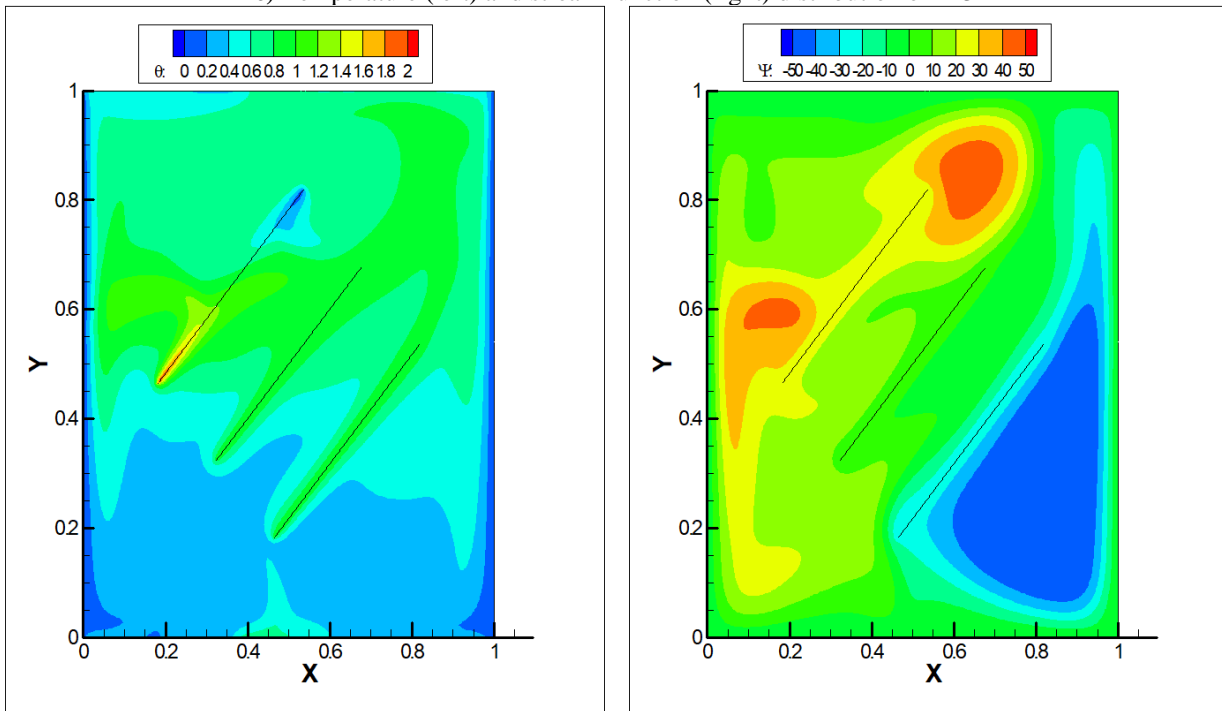
a) Temperature (left) and stream function (right) distribution of T-1



b) Temperature (left) and stream function (right) distribution of T-2



c) Temperature (left) and stream function (right) distribution of T-3



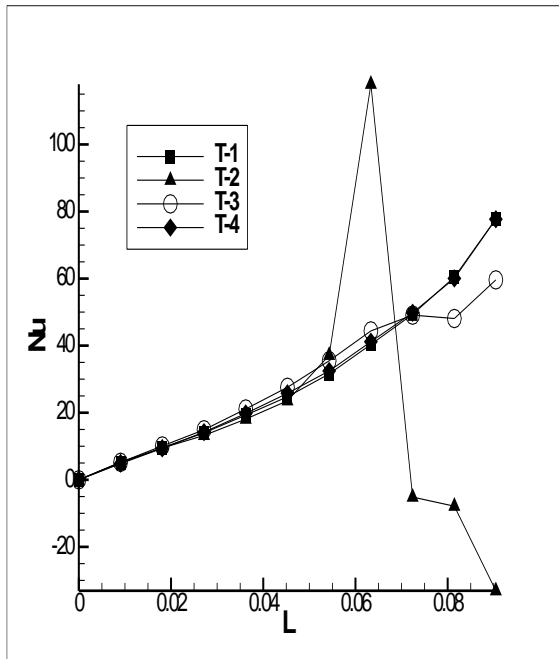
d) Temperature (left) and stream function (right) distribution of T-4

Fig.11- Temperature and stream function contour of the tilted plates.

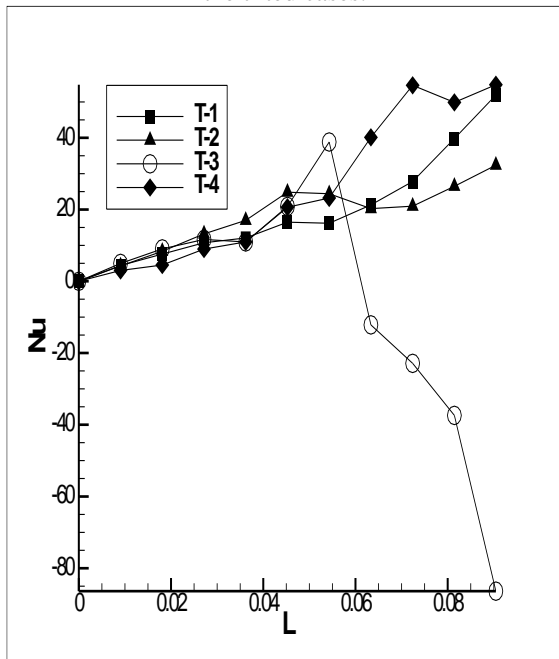
In Fig.12 the local Nu number of the plates has been presented. It is evident that when a non-uniform temperature distribution is applied to one of the plates at a certain position local Nu number decreases sharply. However, an important observation is that the amount of drop of the lower plate is less significant compared to that of the

horizontal and vertical case. In addition, when a non-uniform temperature distribution is applied to one of the plates the local Nu number first rises to a primary maximum amount and then hits its negative peaks. This observation can be understood better by considering the isotherms. As shown, in all of the cases a local temperature

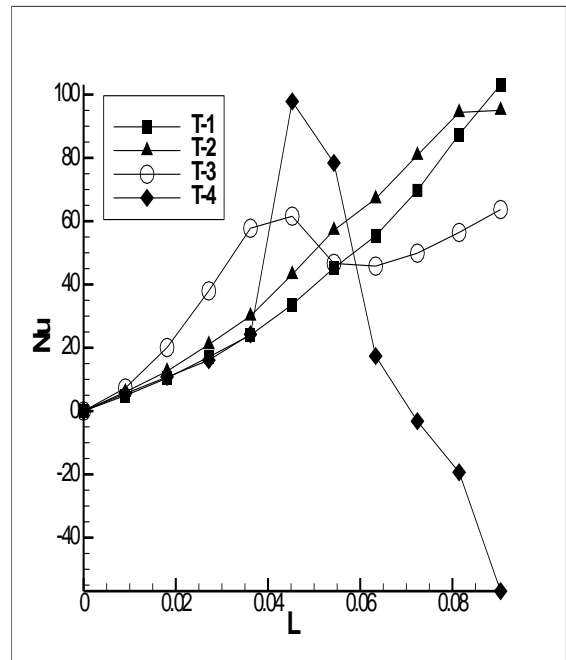
gradient is observed on the non-uniformly heated plate.



a) Local Nusselt number variation of the lower plate in the tilted cases.



b) Local Nusselt number variation of the middle plate in the tilted cases



c) Local Nusselt number variation of the upper plate in the tilted cases

Fig.12- Local Nu number of the tilted case.

In Fig.13 the average Nu number of the tilted case has been presented. As it is observed, in the T-1 case, the upper plate followed by the lower plate experienced the highest amount of average Nu number. Unlike the previous cases, in this case, the introduction of uneven temperature distribution does not necessarily lead to average Nu growth. For instance, in the T-2 case the average Nu number lower plate plummets to its lowest value, while the Nu number of the upper plate rises to its highest amount. The same trend is observed for the upper plate as in the T-4 case average Nu number hits its lowest amount, whereas the Nu number of the lower plate sees an increase.



Fig.13- Average Nu number of the cases T-1 to T-4.

Conclusion

In conclusion, considering the three cases, all cases are separated due to the temperature difference. The main separation mechanism in the horizontal cases is vortex stretching which is mainly present in the area between the plates and results in the most intense local Nu drop. On the other hand, in the vertical convective flow, separation occurs out of the area among the plates. However, both mechanisms are active but not intense in the tilted case. As a result, the local Nu drop is not as sharp as the horizontal case. Therefore, Nu number variation is an intermediate value between the two other cases. This intermediate variation in the local Nu number of tilted plates can be regarded as the main characteristic of this case. Moreover, in the T-4 case, the main part of the convective flow is

present in the area between the middle and the upper plate. Furthermore, another characteristic of the tilted case is the primary positive peak. In Table 2, a comparison among the cases has been drawn. As seen, the least amount of variation, equal to 1.18, is associated with the vertical case because of the geometrical constraint impeding the vortex stretching phenomenon. Moreover, it was found that the highest amount of variation in Nu number occurs in the horizontal case hitting a peak of 60.24 as the position of the plates allows an easy permeation of the convective flow between the plates. This clearly indicates the importance of plate configuration in a cavity for the aforementioned applications, as the variation in the Nu number may differ up to 60 times for a single plate leading to a sharp thermal stress gradient.

Table 2- comparison of the average Nu number.

case	Plates			
Horizontal	lower	middle	upper	variation
H-1	25.433798	20.194474	31.305669	5.661022
H-2	34.316959	11.129707	15.100656	14.13452
H-3	24.800565	113.95058	22.378275	60.24078
H-4	26.546095	18.730707	25.64913	2.904118
Vertical	middle	right	variation	
V-1	27.702332	25.337337	1.1824972	
V-2	25.771371	17.264467	4.2534521	
V-3	22.648078	27.507332	2.4296269	
Tilted	lower	middle	upper	variation
T-1	33.231752	20.836199	45.106262	12.04819
T-2	27.099059	19.224949	50.759027	18.39801
T-3	31.575584	25.531656	44.739363	10.7905
T-4	33.535956	27.096038	32.99084	2.328345

References

[1]S. Saravanan and C. Sivaraj, "Combined natural convection and thermal radiation in a square cavity with a nonuniformly heated plate," *Comput. Fluids*, vol. 117, pp. 125–138, 2015, doi: 10.1016/j.compfluid.2015.05.005.

[2]O. Prakash and S. N. Singh, "Experimental and numerical study of mixed convection with surface radiation heat transfer in an air-filled ventilated cavity," *Int. J. Therm. Sci.*, vol. 171, no. January 2021, p. 107169, 2022, doi: 10.1016/j.ijthermalsci.2021.107169.

[3]A. Hajatzadeh Pordanjani, S. Aghakhani, A. Karimipour, M. Afrand, and M. Goodarzi, "Investigation of free convection heat transfer and entropy generation of nanofluid flow inside a cavity affected by magnetic field and thermal radiation," *J. Therm. Anal. Calorim.*, vol. 137, no. 3, pp. 997–1019, 2019, doi: 10.1007/s10973-018-7982-4.

[4]S. Nazari, R. Ellahi, M. M. Sarafraz, M. R. Safaei, A. Asgari, and O. A. Akbari, "Numerical study on mixed convection of a non-Newtonian nanofluid with porous media in a two lid-driven square cavity," *J. Therm. Anal. Calorim.*, vol. 140, no. 3, pp. 1121–1145, 2020, doi: 10.1007/s10973-019-08841-1.

[5]L. Yang, W. Ji, M. Mao, and J. nan Huang, "An updated review on the properties, fabrication and application of hybrid-nanofluids along with their environmental effects," *J. Clean. Prod.*, vol. 257, p. 120408, 2020, doi: 10.1016/j.jclepro.2020.120408.

[6]A. H. Pordanjani and S. Aghakhani, "Numerical Investigation of Natural Convection and Irreversibilities between Two Inclined Concentric Cylinders in Presence of Uniform Magnetic Field and Radiation," *Heat Transf. Eng.*,

- vol. 43, no. 11, pp. 937–957, 2022, doi: 10.1080/01457632.2021.1919973.
- [7] S. Rostami *et al.*, “A review on the control parameters of natural convection in different shaped cavities with and without nanofluid,” *Processes*, vol. 8, no. 9, 2020, doi: 10.3390/pr8091011.
- [8] Y. Peng *et al.*, “Investigation of energy performance in a U-shaped evacuated solar tube collector using oxide added nanoparticles through the emitter, absorber and transmittal environments via discrete ordinates radiation method,” *J. Therm. Anal. Calorim.*, vol. 139, no. 4, pp. 2623–2631, 2020, doi: 10.1007/s10973-019-08684-w.
- [9] A. S. Dogonchi, M. S. Sadeghi, M. Ghodrati, A. J. Chamkha, Y. Elmasry, and R. Alsulami, “Natural convection and entropy generation of a nanofluid in a crown wavy cavity: Effect of thermo-physical parameters and cavity shape,” *Case Stud. Therm. Eng.*, vol. 27, p. 101208, 2021, doi: 10.1016/j.csite.2021.101208.
- [10] R. El Ayachi *et al.*, “Numerical Heat Transfer , Part A : Applications An International Journal of Computation and Methodology Combined Effects of Radiation and Natural Convection in a Square Cavity Submitted to Two Combined Modes of Cross Gradients of Temperature,” vol. 7782, no. February 2016, pp. 249–270, 2012, doi: 10.1108/10878571211209314.
- [11] A. Yilcel, S. Acharya, and M. L. Williams, “Natural convection and radiation in a square enclosure,” *Numer. Heat Transf. Part A Appl.*, vol. 15, no. 2, pp. 261–278, 1989, doi: 10.1080/10407788908944688.
- [12] L. El Moutaouakil, M. Boukendil, Z. Zrikem, and A. Abdelbaki, “Natural Convection and Surface Radiation Heat Transfer in a Square Cavity with an Inner Wavy Body,” *Int. J. Thermophys.*, vol. 41, no. 8, pp. 1–21, 2020, doi: 10.1007/s10765-020-02688-7.
- [13] H. Bouali, A. Mezrhab, H. Amaoui, and M. Bouzidi, “Radiation-natural convection heat transfer in an inclined rectangular enclosure,” *Int. J. Therm. Sci.*, vol. 45, no. 6, pp. 553–566, 2006, doi: 10.1016/j.ijthermalsci.2005.10.001.
- [14] V. Vivek, A. K. Sharma, and C. Balaji, “Interaction effects between laminar natural convection and surface radiation in tilted square and shallow enclosures,” *Int. J. Therm. Sci.*, vol. 60, pp. 70–84, 2012, doi: 10.1016/j.ijthermalsci.2012.04.021.
- [15] C. Shu, H. Xue, and Y. D. Zhu, “Numerical study of natural convection in an eccentric annulus between a square outer cylinder and a circular inner cylinder using DQ method,” *Int. J. Heat Mass Transf.*, vol. 44, no. 17, pp. 3321–3333, 2001, doi: 10.1016/S0017-9310(00)00357-4.
- [16] M. Jami, A. Mezrhab, M. Bouzidi, and P. Lallemand, “Lattice Boltzmann method applied to the laminar natural convection in an enclosure with a heat-generating cylinder conducting body,” *Int. J. Therm. Sci.*, vol. 46, no. 1, pp. 38–47, 2007, doi: 10.1016/j.ijthermalsci.2006.03.010.
- [17] F. Garoosi, F. Hoseinnejad, and M. M. Rashidi, “Numerical study of natural convection heat transfer in a heat exchanger filled with nanofluids,” *Energy*, vol. 109, pp. 664–678, 2016, doi: 10.1016/j.energy.2016.05.051.
- [18] H. S. Yoon, M. Y. Ha, B. S. Kim, and D. H. Yu, “Effect of the position of a circular cylinder in a square enclosure on natural convection at Rayleigh number of 107,” *Phys. Fluids*, vol. 21, no. 4, 2009, doi: 10.1063/1.3112735.
- [19] O. Zeitoun and M. Ali, “Numerical investigation of natural convection around isothermal horizontal rectangular ducts,” *Numer. Heat Transf. Part A Appl.*, vol. 50, no. 2, pp. 189–204, 2006, doi: 10.1080/10407780600604958.
- [20] J. Sieres, A. Campo, E. H. Ridouane, and J. Fernández-Seara, “Effect of surface radiation on buoyant convection in vertical triangular cavities with variable aperture angles,” *Int. J. Heat Mass Transf.*, vol. 50, no. 25–26, pp. 5139–5149, 2007, doi: 10.1016/j.ijheatmasstransfer.2007.07.006.
- [21] M. Sheikholeslami, D. D. Ganji, and M. M. Rashidi, “Ferrofluid flow and heat transfer in a semi annulus enclosure in the presence of magnetic source considering thermal radiation,” *J. Taiwan Inst. Chem. Eng.*, vol. 47, pp. 6–17, 2015, doi: 10.1016/j.jtice.2014.09.026.
- [22] A. Bahlaoui, A. Raji, M. Hasnaoui, M. Naïmi, T. Makayssi, and M. Lamsaadi, “Mixed convection cooling combined with surface radiation in a partitioned rectangular cavity,” *Energy Convers. Manag.*, vol. 50, no. 3, pp. 626–635, 2009, doi: 10.1016/j.enconman.2008.10.001.
- [23] T. Basak, S. Roy, and A. R. Balakrishnan, “Effects of thermal boundary conditions on natural convection flows within a square cavity,” *Int. J. Heat Mass Transf.*, vol. 49, no. 23–24, pp. 4525–4535, 2006, doi: 10.1016/j.ijheatmasstransfer.2006.05.015.
- [24] M. Corcione, “Effects of the thermal boundary conditions at the sidewalls upon natural convection in rectangular enclosures heated from below and cooled from above,” *Int. J. Therm. Sci.*, vol. 42, no. 2, pp. 199–208, 2003, doi: 10.1016/S1290-0729(02)00019-4.
- [25] C. Cianfrini, M. Corcione, and P. P. Dell’Omo, “Natural convection in tilted square cavities with differentially heated opposite walls,” *Int. J. Therm. Sci.*, vol. 44, no. 5, pp. 441–451, 2005, doi: 10.1016/j.ijthermalsci.2004.11.007.
- [26] R. El Ayachi, A. Raji, M. Hasnaoui, and A. Bahlaoui, “Combined effect of radiation and natural convection in a square cavity differentially heated with a periodic temperature,” *Numer. Heat Transf. Part A Appl.*, vol. 53, no. 12, pp. 1339–1356, 2008, doi: 10.1080/10407780801960043.
- [27] E. H. Ridouane, M. Hasnaoui, A. Amahmid, and A. Raji, “Interaction between natural convection and radiation in a square cavity heated from below,” *Numer. Heat Transf. Part A Appl.*, vol. 45, no. 3, pp. 289–311, 2004, doi: 10.1080/10407780490250373.
- [28] M. Kim, J. H. Doo, Y. G. Park, H. S. Yoon, and M. Y. Ha, “Natural convection in a square enclosure with a circular cylinder according to the bottom wall temperature variation,” *J. Mech. Sci. Technol.*, vol. 28, no. 12, pp. 5013–5025, 2014, doi: 10.1007/s12206-014-1123-1.

COPYRIGHTS

©2023 by the authors. Published by Iranian Aerospace Society This article is an open access article distributed under the terms and conditions of the Creative Commons Attribution 4.0 International (CC BY 4.0)

<https://creativecommons.org/licenses/by/4.0/>.

